Available online at www.sciencedirect.com
ScienceDirect
Polyhedron 26 (2007) 958–966
POLYHEDRON
www.elsevier.com/locate/poly

The synthesis of a new dithiophosphonic acid and its coordination properties toward Ni(II): A combined NMR and X-ray diffraction study

E. Alberti, G.A. Ardizzoia, S. Brenna, F. Castelli, S. Galli *, A. Maspero *

Dipartimento di Scienze Chimiche e Ambientali, Università degli Studi dell'Insubria, via Valleggio 11, 22100 Como, Italy

Received 3 August 2006; accepted 22 September 2006
Available online 4 October 2006

Abstract

In order to investigate the coordination properties of the new, dianionic, S-donor ligand 4-methoxophenyldithiophosphonate (L), a dithiophosphonate salt of $L(H_2pz)_2$ formula was prepared (Hpz = pyrazole), characterized by multinuclear solution and solid state NMR, and subsequently employed in the synthesis of two Ni(II) metal complexes of $[NiL_2](H_2pz)_2$ and $[NiL_2](HNEt_3)_2$ formula. The latter species were fully characterized by a combined NMR and X-ray diffraction study, allowing to disclose interesting structural features, such as subtle deformations of the ligand (and their influence on the magnetic resonance properties of the ^{31}P nuclei), imposed by distinct hydrogen-bond patterns.

Keywords: Lawesson reagent; Dithiophosphonate; Nickel complexes; CPMAS NMR; Crystal structure

1. Introduction

Thiophosphorus species are an important class of S-donor ligands. This category includes dithiophosphate, dithiophosphonate and dithiophosphinate compounds (**1**, **2** and **3**, respectively, see Scheme 1), which are used in a variety of applications in the agricultural and industrial fields, as insecticides [1,2], nematocides [3,4], or as antioxidants in lubricants and plastics [5,6]. These compounds are also versatile ligands, displaying a broad variety of coordination patterns leading to a great diversity of molecular and supramolecular structures [7,8]. Even some of their metal derivatives are industrially employed as lubricants and additives [9,10]. In addition, dithiophosphonate complexes are known to possess biologically relevant properties [11]. Generally, thiophosphorus ligands are not commercially available: several scientific reports on their synthesis have appeared [12]. Dithiophosphates, **1**, and dithiophosphonates, **2**, can be easily synthesized starting from the Lawesson's dimer $[S_2P(p\text{-}C_6H_4OMe)]_2$ [13] (**4**, see Scheme 2), since, under suitable conditions, it can give a ring opening reaction by nucleophilic attack. Even though the synthesis and characterization of thiophosphorus ligands and of a few transitions metal derivatives have been deeply investigated, very little is known on the chemistry of dithiophosphonic acids. Accordingly, the first metal complexes of dithiophosphonates have been reported only recently [14].

Our interest in the coordination chemistry of dithiophosphonate ligands [15] boosted us to investigate the synthesis and characterization of a new, dianionic, S-donor ligand, 4-methoxophenyldithiophosphonate (L), and its coordination properties towards d^8 transition metals. In the following, we thus present a convenient synthetic way for preparing dithiophosphonate derivatives, such as the $L(H_2pz)_2$ salt (**5**, Hpz = pyrazole), and its Ni(II) metal complexes $[NiL_2](H_2pz)_2$ (**7**) and $[NiL_2](HNEt_3)_2$ (**8**). Their interesting structural features were addressed by a combination of single crystal and powder X-ray diffraction with multinuclear solution and solid state NMR.

* Corresponding authors.
E-mail address: angelo.maspero@uninsubria.it (A. Maspero).

0277-5387/$ - see front matter © 2006 Elsevier Ltd. All rights reserved.
doi:10.1016/j.poly.2006.09.077

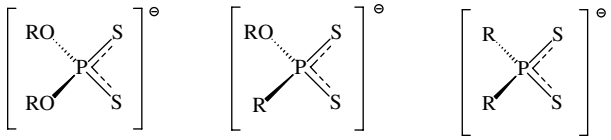

Dithiophosphate, 1 **Dithiophosphonate, 2** **Dithiophosphinate, 3**

Scheme 1.

2. Results and discussion

2.1. Synthesis, characterization and solution properties of species 5 and 6

When a suspension of the Lawesson's dimer $[S_2P(p\text{-}C_6H_4OMe)]_2$ (**4**, Scheme 2) in toluene was treated under nitrogen with a large excess of pyrazole (Hpz), a white precipitate formed (**5**, Scheme 3, pathway 1), which, on the basis of elemental analysis, IR and multinuclear spectroscopy, was formulated as an adduct between pyrazole and dithiophosphonic acid (H_2L), with $H_2L \cdot 2Hpz$ formula. Nevertheless, the presence of multiple bonding sites for the acidic proton [the N site(s) on the pz moiety and the S or O sites on the dithiophosphonate ligand] cannot rule out the presence of different tautomers, such as a bispyrazolium salt, $L(H_2pz)_2$, or even a species where the hydrogen atoms are extensively shared between the above quoted N, O and S acceptors.[1]

Species **5** was found to transform from a white solid into a dense liquid if left in air. Why this occurs it is not clear. X-ray powder diffraction (XRPD) indicated the solid to be highly crystalline; yet, as observed by performing a profile fitting of time-dependent XRPD traces, the decomposition has a $t_{1/2}$ value just above 4 h (Fig. 1). GC–MS measurements of the evolved gas fraction did not support any conclusive information, thus leaving the question still open. The XRPD crystalline trace (collected in conventional Bragg–Brentano mode in the air) is nevertheless too complex for an ab initio structural analysis; *inter alia*, this agrees with the presence of two formula units in the asymmetric unit of the crystals, as evidenced by solid state ^{31}P NMR (vide infra). The IR spectrum of solid **5**, recorded in nujol mull, shows a broad absorption at 1869 cm^{-1}, which is likely due to strong hydrogen bonds of the P–O–H–N kind, involving the dithiophosphonic acid and the heteroaromatic ring.

The ^{31}P NMR spectrum of **5** in acetone-d_6 shows one singlet centred at 78.6 ppm (see Table 1). This value shows an upfield shift of about 30 ppm compared to that found earlier for dithiophosphonate ligands [15,16], suggesting the presence of a relatively highly charged (dianionic) form of L for **5**, thus supporting, at least in solution, the formulation of **5** as a bispyrazolium salt, $L(H_2pz)_2$. On lowering the temperature down to 183 K, the ^{31}P NMR spectrum shows only one broader peak at 86.2 ppm, indicating that the system is in the fast exchange regime at room temperature (RT) and that the exchange rate decreases only slightly at low temperature. Unfortunately, the corresponding low temperature ^1H NMR spectrum cannot be employed to follow in detail this process, due to the complexity of the signals in the aromatic region. At room temperature, the ^1H NMR spectrum of **5** (in acetone-d_6) shows two multiplets at 7.9 and 7.1 ppm due to the protons of the aryl group, one singlet centred at 3.8 ppm for the OMe residue and

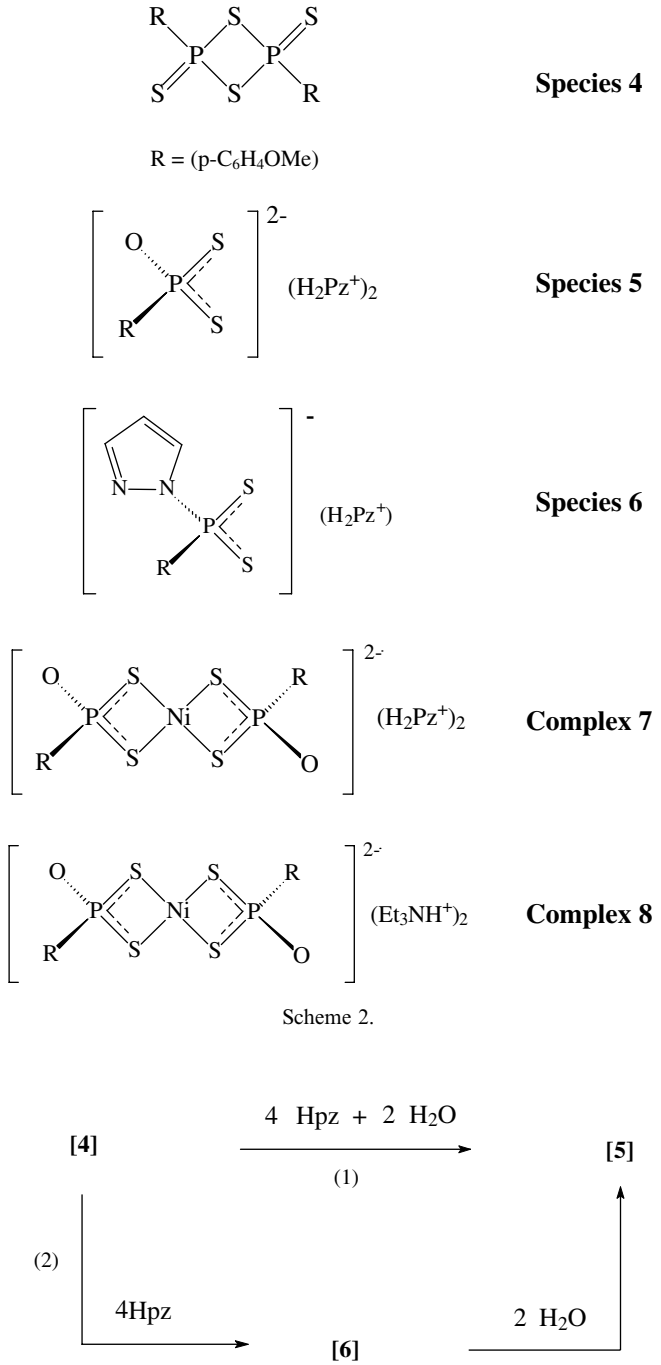

Species 4

R = (p-C_6H_4OMe)

Species 5

Species 6

Complex 7

Complex 8

Scheme 2.

Scheme 3.

[1] For the sake of completeness, it must be said that even a formulation of the $[(MeO)C_6H_4\text{–}PS_2\text{–}O\text{–}PS_2\text{–}C_6H_4(OMe)](Hpz)_2(H_2pz)_2$ kind cannot be excluded (*Anal.* Calc.: C, 44.95; H, 4.64; N, 16.13), being it consistent even with the ^{31}P CPMAS NMR evidences.

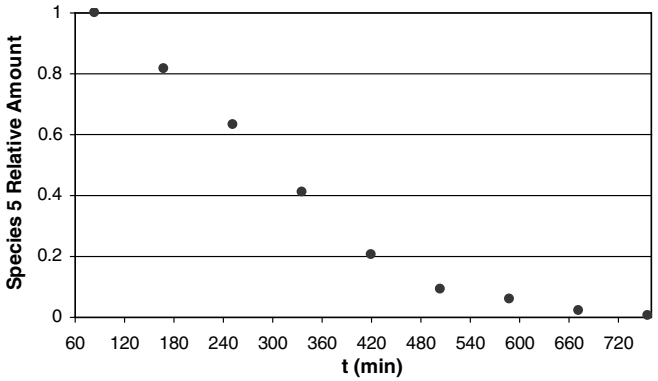

Fig. 1. Time dependence of the solid to liquid decomposition of the (polycrystalline) species **5** if left in air at RT, as followed by the disappearance of the pertinent peaks in the powder diffraction traces.

Table 1
^{31}P chemical shifts (ppm) for species **5**–**8**

Sample	^{31}P solution[a]	^{31}P CPMAS	^{31}P SPE
Species **5**	78.6	97.3	97.3
		94.5	94.5
Species **5** quenched	78.0	97.3	97.2
		94.5	94.4
			89.9
Species **6**	72.8		
Species **6**[*]	78.1	97.2	97.1
	72.8	94.4	94.4
			82.3
Complex **7**	85[b]	77.3	
Complex **8**	69.4[c]	59.7	

[*] Recrystallized from anhydrous toluene (see text).
[a] Spectra recorded in acetone.
[b] Broad peak.
[c] Spectra recorded in methanol.

two signals at 7.7 and 6.3 ppm, assigned to the protons of the pyrazole moiety. The assignment of the signal at 10.3 ppm to acidic (N–H) protons [17] was confirmed by its disappearance after isotopic exchange with D_2O.

The formulation of **5** was also confirmed by the ^{13}C NMR spectrum (recorded at RT in acetone) which shows, beside the phenyl C-atoms signals, only two resonances for the heterocycle at 105.0 and 133.6 ppm, attributed to C(4) and C(3)/C(5), respectively. This excludes any possibility of a P–N bound species.

On the basis of these spectral observations, intermolecular hydrogen bonds between the adducts can be ruled out in solution and, taking into account the elemental analysis, the presence of two molecules of pyrazole *per* molecule of dithiophosphonic acid is implicit.

The fact that no pyrazolium *N*-pyrazolyl-4-methoxyphenyl-phosphonamidodithiolate was obtained when pyrazole alone was reacted with the Lawesson's reagent is here attributed to the specific electron properties of this heterocycle. Indeed, pyrazole can be considered a "hybrid" molecule, the lone pair on N(2) making it nucleophilic, while its aromatic nature transforming it into a good leaving-group.

In order to investigate the role played by Hpz in the reaction with **4**, a new synthesis was carried out in anhydrous conditions. It is well known that aliphatic amines readily react with the Lawesson's dimer forming a stable P–N bond [18]. Accordingly, when a solventless reaction between the Lawesson's reagent and an excess of pyrazole was carried out at 343 K and under nitrogen atmosphere, a new derivative, **6**, could be isolated. Species **6** was formulated as a 4-methoxy-phenylphosphonoaminodithiolate pyrazolium salt (Scheme 2), on the basis of multinuclear NMR spectroscopy. The RT ^{31}P NMR spectrum of **6** recorded in acetone-d_6 shows a sharp signal centred at 72.8 ppm in agreement with the presence of a phosphorus atom directly bound to a nitrogen one [18,19]. In the presence of water, or moisture, compound **6** hydrolyzes very quickly and species **5** is immediately formed, as confirmed by the ^{31}P NMR spectrum of **6**, recorded (in acetone-d_6) after addition of few drops of water and under nitrogen: the latter spectrum shows, beside the signal due to the N-bound P atom, a new peak centred at 78.1 ppm, i.e. that of the phosphorous atom of the P–O bound species **5**. After 30 min, only the signal centred at 78.1 ppm can be observed. This spectroscopic evidence suggests that the first step of the reaction between **4** and pyrazole is the ring opening reaction by nucleophilic attack of the heterocycle to the Lawesson's reagent with the formation of **6**. In the presence of water, the labile species **6** hydrolyzes quickly, forming the more stable derivative **5** (see Scheme 3, pathway 2). The proposed chemical nature of **6** was also confirmed by ^{31}P solid state NMR spectroscopy, as described below.

2.2. Solid state NMR characterization of species 5 and 6

In the absence of samples suitable for conventional X-ray diffraction studies, species **5** and **6** were analysed by solid state NMR spectroscopy, in order to gain some structural information. The ^{31}P CPMAS spectrum of **5** (Fig. 2a, Table 1) shows two distinct peaks at 97.3 ppm and 94.5 ppm, with a downfield shift of about 20 ppm with respect to the single resonance observed in the NMR spectrum in solution (78.6 ppm in acetone). This different chemical shift between the spectra in the solid state and in solution may depend on packing effects, likely the presence of intermolecular hydrogen bonds between the dithiophosphonic acid and the pyrazole.

The chemical shifts of the peaks in the solid state are in agreement with previous studies [19] which report P–O signals resonating in the range 95–110 ppm. The splitting of the ^{31}P signal into two peaks is confirmed by the ^{13}C CPMAS spectrum (Fig. 2b), in which the isolated signals of the O-methyl (at about 55 ppm) and the P-*ipso* (about 160 ppm) carbon nuclei are split into two peaks each. Unfortunately, the extreme peak overlapping in the aromatic region does not allow to unambiguously assign the pyrazole signals. However, it is well known that, in the solid state, pyrazole gives three distinct peaks at

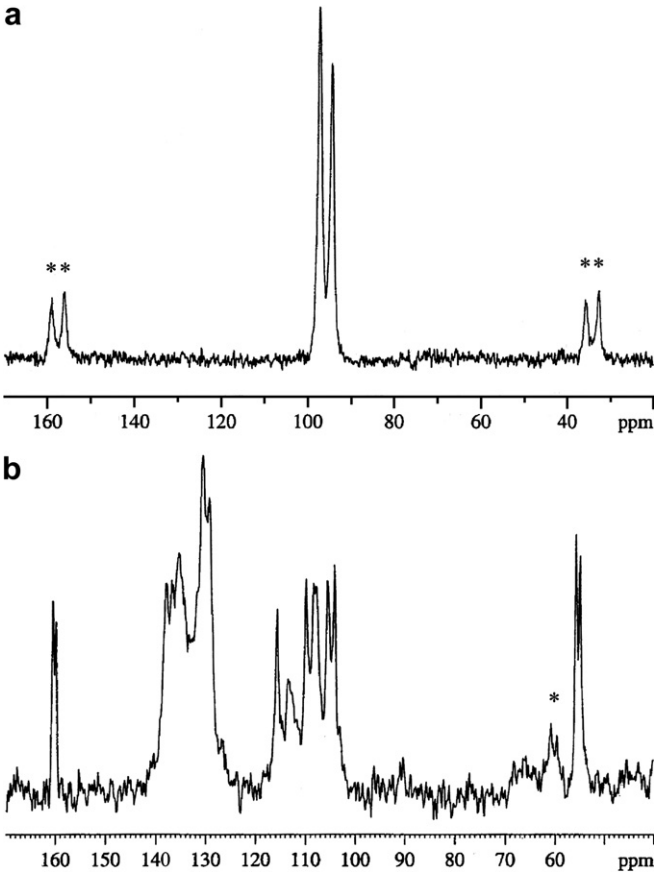

Fig. 2. Solid state NMR spectra of **5**: (a) ^{13}C CPMAS, Number of scans (NS) = 820. (b) ^{31}P CPMAS, NS = 20. Asterisks indicate spinning sidebands.

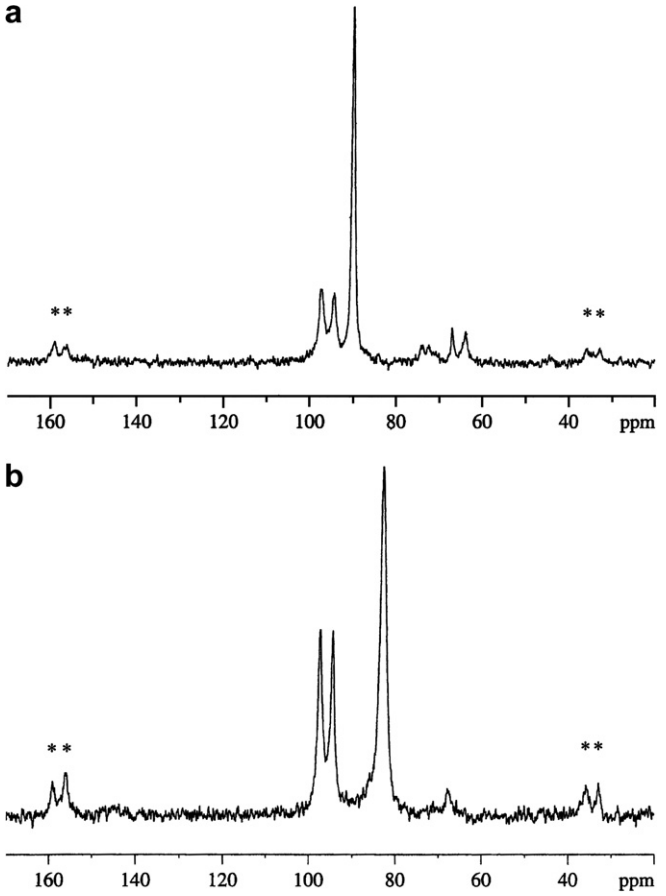

Fig. 3. ^{31}P SPE experiment with recycle delay of 5 s for (a) **5** quenched, Number of scans (NS) = 164, (b) **6***, NS = 48. Asterisks indicate spinning sidebands.

138.7 ppm (C3), 107.0 ppm (C4) and 128.8 ppm (C5) ppm [20]. The clear absence of peaks in the 128 ppm region in the spectrum of **5** seems to indicate that no ''free'' pyrazole is present in species **5**, thus suggesting, in agreement with the above IR results, the presence of a network of hydrogen bonds in the solid.

The presence of split ^{31}P and ^{13}C peaks may suggest either the occurrence of two different phosphorous chemical environments coexisting in a single crystalline phase, or the co-presence of different crystalline forms within the sample. On the basis of the relative intensities of the two peaks (approximately 1:1) the first hypothesis seems more likely. The existence of two crystalline forms in the sample is ruled out by a further experiment in which **5** is obtained by rapidly quenching the reaction mixture down to 273 K before filtering. The ^{31}P CPMAS spectrum recorded on this product was identical to that of species **5**, whereas the ^{31}P SPE spectrum registered with a short recycle delay shows an additional peak at 89.9 ppm (Fig. 3a). The SPE experiment is known to enhance the resonance of those nuclei with a short relaxation time, T_{1P}, i.e. phosphorous nuclei possessing distinct dynamics from those responsible for the peaks in the CPMAS spectrum (in the present case, the two peaks at 97.3 ppm and 94.5 ppm). We suggest that the new peak at 89.9 ppm may belong to an amorphous phase, the formation of which is favoured upon fast cooling and, as expected, is absent in the ^{31}P SPE spectrum of **5** obtained upon slow crystallization. Besides, the presence of the two peaks at 97 and 94 ppm with similar relative intensity, supports the exclusion of the concomitant existence of two crystalline phases.

With the purpose of characterizing the P–N bound species by solid state NMR, **6** was recrystallized using anhydrous toluene, thus changing the consistency of the sample from a sticky material to a solid suitable to be packed in the NMR rotor, **6***. The ^{31}P CPMAS spectrum (not reported) shows two peaks centred at 97.2 ppm and 94.4 ppm, assigned to **5**, which is quickly formed by hydrolysis of **6**. However, an additional peak at 82.2 ppm was found in the ^{31}P SPE spectrum (Fig. 3b), which, on the basis of its chemical shift value [19], is assigned to a phosphorous nucleus of the P–N bound species **6**, thus corroborating the existence of an intermediate P–N species.

2.3. Synthesis and spectroscopic characterization of species 7 and 8

Although both derivatives **5** and **6** can be considered flexible multitopic ligands, the low stability of **6** pushed

us to investigate the coordination properties of species **5** only.

When a suspension of **5** in acetonitrile was treated with $Ni(ClO_4)_2 \cdot 6H_2O$, a violet compound formed, which, on the basis of elemental analysis and spectroscopic data, was formulated as $[NiL_2](H_2Pz)_2$ (**7**). The IR spectrum of **7** (nujol mull) shows one broad band at 1870 cm^{-1}, due to the presence of strong hydrogen bonds of the P–O–H–N kind (as substantiated by the complete structure determination, vide infra).

The RT ^{31}P NMR spectrum of **7** in solution presents one broad peak centred at about 85 ppm, while, on lowering the temperature at 183 K, two sharp peaks at 82.0 and 80.4 ppm appear, suggesting that at low temperatures a slow exchange regime is reached. This fluxional property of **7** may be assigned to the interconversion of the *cis* and *trans* isomers [15].

The RT ^1H NMR spectrum of **7** shows two multiplets centred at 8.1 and 7.1 ppm (phenyl protons), a singlet at 3.9 ppm (methoxo protons) and one broad peak at 4.2 ppm, attributed to an acidic proton. At RT, the protons of pyrazole are undetectable, probably because their signals are so broad to be hidden in the baseline, suggesting an intermediate exchange rate for pyrazole. At 163 K, the ^1H NMR spectrum of **7** shows new signals: one triplet centred at 6.5 ppm, and one doublet at 8.1 ppm, assignable to the protons of the heteroaromatic ring. This indicates that the fluxional process involving pyrazole is substantially slowed down at 163 K. A fundamental role in lowering the rate of the fluxional process may be played by the possibility of formation of strong hydrogen bonds (of P–O–H–N type) even in solution. This was indeed confirmed by the fact that, at RT, after addition of few drops of deuterium oxide, the pyrazole signals do appeared. Apparently, the presence of ^2H versus ^1H nuclei slows down the fluxional process, as does lowering the temperature. Similar isotopic effects have been recently reviewed [21].

On the other hand, when the reaction between **5** and $Ni(ClO_4)_2 \cdot 6H_2O$ was carried out in the presence of triethylamine, a brown precipitate formed, which, on the basis of elemental analysis, IR and ^1H NMR spectroscopy, was formulated as $[NiL_2](Et_3NH)_2$ (**8**), as confirmed by the single crystal X-ray diffraction characterization described below. Species **8** can also be obtained starting from **7** in the presence of triethylamine, showing the stronger basicity of the tertiary amines versus pyrazole.

The RT ^{31}P NMR spectrum of **8** in methanol-d_4 shows one singlet centred at 69.4 ppm while, lowering the temperature at 173 K, two sharp peaks at 73.7 and 72.2 ppm appear. Analogously to what observed for **7**, a slow exchange regime is reached at 173 K, which allows to detect the interconversion process between the *cis* and *trans* isomers.

The RT ^1H NMR spectrum of **8** registered in acetone-d_6 shows two multiplets centred at 8.3 and at 6.7 ppm (aromatic protons), one singlet at 3.8 ppm (methoxo group), and two multiplets centred at 3.2 and 1.3 ppm, due to the triethylamonium ion. On lowering the temperature down to 173 K, these spectral features do not change.

The ^{31}P CPMAS spectra for both nickel complexes **7** and **8** show single peaks at 77.3 ppm and 59.7 ppm, respectively. This large chemical shift difference can be in principle attributed to two distinct, but possibly convergent, effects: the strength of the P–O–H–N interactions, and the electronic reorganization within the RPS_2O fragments, with different hybridization and double bond character of the P=O bond. These subtle effects will be further considered when discussing the X-ray diffraction results (vide infra). The finding of an individual peak for both complexes indicates that only one phosphorus environment is present in the structure, and that the complex must lie about a crystallographic symmetry element. This also suggests that both species crystallize in a unique isomeric form, also in agreement with the crystallographic features which identify the *trans* isomer.

2.4. Crystal and molecular structure of species 7 and 8

Both complexes **7** and **8** crystallize in the triclinic space group $P\bar{1}$. The asymmetric unit of the former species comprises half a Ni(II) ion, lying about a crystallographic inversion centre, one phosphodithiolate ligand (L) and one pyrazole moiety. Whether the latter is a true neutral Hpz molecule, a pyrazolium cation (H_2pz^+) or an intermediate form is not relevant, since an extended network of hydrogen-bonds shows that the acidic hydrogen atoms are shared, in the solid, in the different D–H···A wells.

Also in species **8**, a centrosymmetric $[NiL_2]^{2-}$ complex is present, hydrogen-bonded to one triethylammonium cation on each side. As can be appreciated in Figs. 4 and 5, in both **7** and **8**, the metal centre is tetracoordinated in square planar geometry by four sulfur atoms belonging to two distinct L ligands. Thus, in both compounds, the L moiety acts as a S,S′-chelating ligand, promoting comparable Ni–S bonds of about 2.22 Å and similar S–Ni–S angles of about 88° and 92° (Table 2). Within both $[NiL_2]^{2-}$ complexes, the 4-methoxyphenyl and oxo substituents on each phosphorous atom adopt a *trans* disposition with respect to the mean plane individuated by the NiS_2P_2 moiety, in agreement with the ^{31}P CPMAS NMR observations of a unique isomer and magnetically equivalent P nuclei.

In **7**, the pyrazole ligand is not coordinated to the metal centre. Nevertheless, both nitrogen atoms are involved in hydrogen bond interactions of about 2.65 Å with the oxo substituents of L ligands belonging to two distinct, adjacent $[NiL_2]^{2-}$ complexes (Fig. 6). The presence of such a hydrogen bond implies a slight (yet statistically significant) lengthening of the P–O bond distance, being 1.538(2) Å in complex **7** versus 1.502(2) Å in **8**. It is worth noting that even in species **8** the oxo substituent is involved in a hydrogen bond interaction of about 2.7 Å with the nitrogen atom of an adjacent triethylammonium cation. The different number (and type) of P=O–H–N bonds in **7** and **8** (Table 1) thus affects the local electronic distribution at the P=O

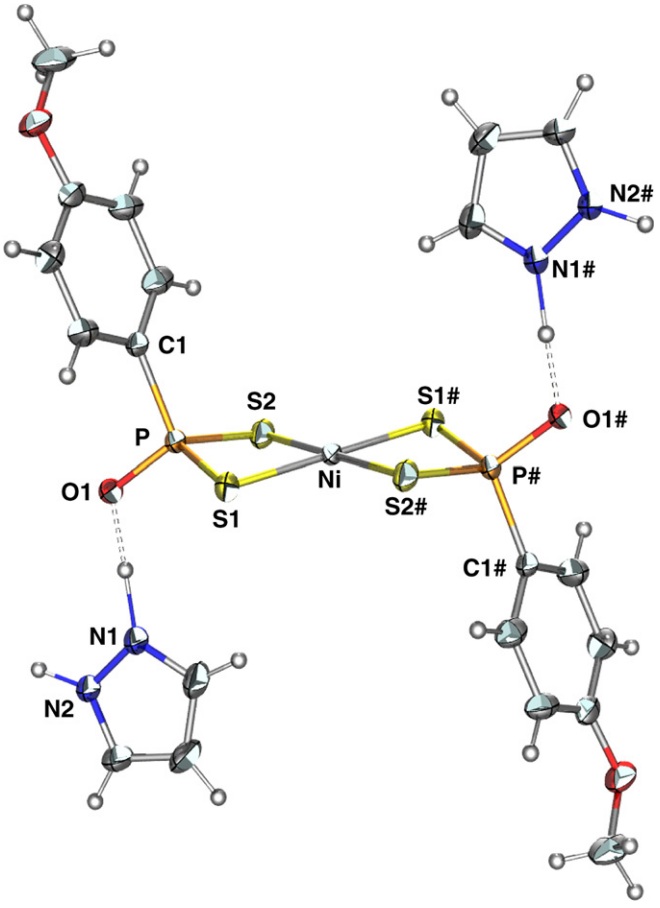

Fig. 4. ORTEP representation (30% probability level) of the molecular structure in complex **7**. Carbon, grey; hydrogen light grey; nitrogen, blue; oxygen, red; phosphorous, orange; sulfur, yellow; nikel, grey. The N–H···O hydrogen bonds between the $[NiL_2]^{2-}$ anion and the pyrazole ligands have been depicted through dashed lines (both the hydrogen atoms involved in this interaction have been arbitrarily assigned to the nitrogen atoms of the pyrazole ligand). #: $[-x, -y, -z]$. (For interpretation of the references to colour in this figure legend, the reader is referred to the web version of this article.)

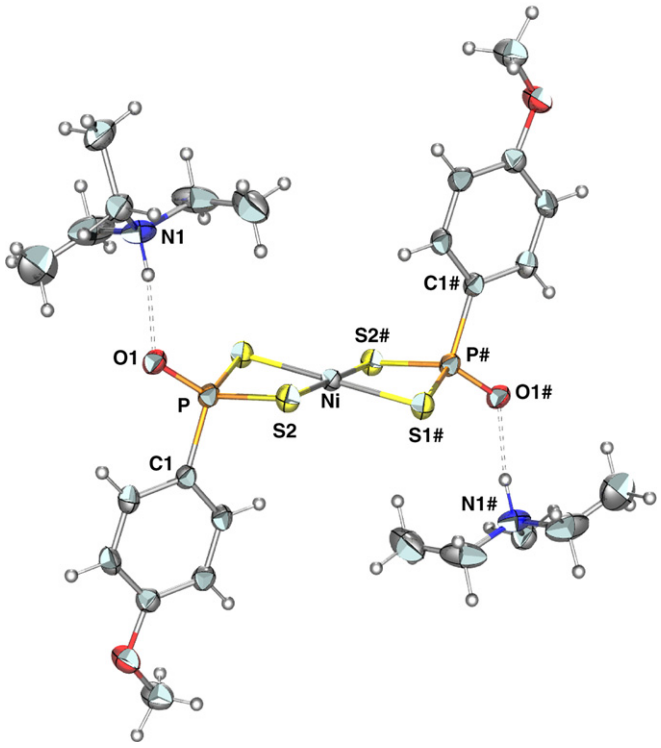

Fig. 5. ORTEP representation (30% probability level) of the $[NiL_2]$-$(HNEt_3)$ moiety present in complex **8**. Carbon, grey; hydrogen light grey; nitrogen, blue; oxygen, red; phosphorous, orange; sulfur, yellow; nickel, grey. The N–H···O hydrogen bond interactions between the $[NiL_2]^{2-}$ anion and the triethylammonium cations have been depicted through dashed lines. The labelling scheme used throughout the manuscript is highlighted. #: $[-x, -y, -z]$. (For interpretation of the references to colour in this figure legend, the reader is referred to the web version of this article.)

fragment; this is also counterbalanced by the slight lengthening (ca. 0.01 Å, i.e. 10σ) of the P–S bonds; these subtle effects may be likely considered responsible for the downfield shift of the ^{31}P peak in the CPMAS spectrum of **7** (with respect to that of **8**), as mentioned above.

As appreciable in Fig. 6, and thanks to the ditopic nature of the pyrazolium cations, the intermolecular interactions present in **7** generate monodimensional chains running in the [1 0 1] direction. At variance, no extended network can exist in **8** and centrosymmetric molecules surrounded each by two triethylammonium cations are present.

3. Experimental

3.1. Materials and methods

Pyrazole (HPz), Lawesson's reagent and salts were used as supplied (Aldrich Chemical Co.). Solvents were dried and distilled by standard methods. All preparations and manipulations were carried out under dinitrogen atmosphere using conventional Schlenk techniques. *Caution:* Perchlorate salts in the presence of transition metal ions

Table 2
Relevant bond distances (Å) and angles (°) for species **7** and **8**

Parameter	7	8
Ni–S1	2.2205(8)	2.218(1)
Ni–S2	2.2243(9)	2.223(1)
P–S1	2.022(1)	2.032(1)
P–S2	2.019(1)	2.031(1)
P–O1	1.538(2)	1.502(2)
P–C1	1.802(3)	1.811(3)
N···O	2.657(3), 2.639(5)	2.689(4)
S1–Ni–S2	87.86(3), 92.14(3)	87.66(4), 92.34(4)
S1–P–S2	99.48(5)	98.36(5)
S1–P–O1	113.91(1)	116.3(1)
S2–P–O1	115.8(1)	116.2(1)
O1–P–C1	106.0(1)	107.7(1)
S1–P–C1	111.1(1)	108.7(1)
S2–P–C1	110.6(1)	109.0(1)
N–H···O	174(4), 177(9)	172(3)

For the labelling scheme, see Figs. 3 and 4.

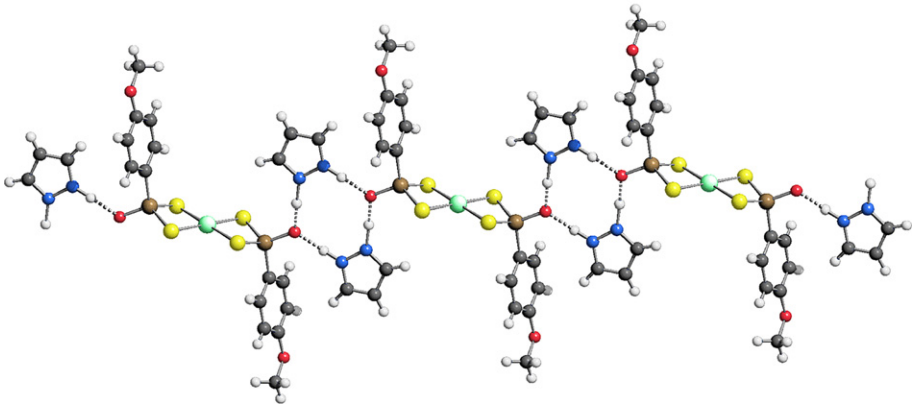

Fig. 6. Schematic representation of the monodimensional chains created by the hydrogen bond interactions (dashed lines) in complex **7**. Carbon, grey; hydrogen light grey; nitrogen, blue; oxygen, red; phosphorous, brown; sulfur, yellow; nickel, light green. (For interpretation of the references to colour in this figure legend, the reader is referred to the web version of this article.)

and organic material are potentially explosive and should be handled with care!

Infrared spectra were recorded on a Shimadzu Prestige-21 instrument. Elemental analyses were carried out on a Perkin–Elmer CHN Analyzer 2400 series II.

NMR spectra were recorded using a Bruker ADVANCE 400 spectrometer, employing for solid state experiments a 4 mm double bearing MAS probe. The standard ^{1}H, ^{13}C and ^{31}P spectra in solution were carried out in acetone (methanol for **8**) at room temperature. For the solid samples ^{31}P cross-polarization magic-angle spinning (CPMAS) spectra were recorded using a recycle time of 4 s, contact times of 1 ms and spinning rates of 10 kHz. ^{31}P single pulse excitation (SPE) experiments with high power proton decoupling were recorded with recycle times of 5 s. The CPMAS experiment select the most hindered carbons, those in the crystalline phase, whereas the SPE experiment acquired with a recycle delay of 5 s selects more mobile carbons (5 s is not enough for complete relaxation of rigid carbons). The ^{31}P spectra were referenced with respect to 85% aqueous H_3PO_4 by setting the ^{31}P NMR peak of poly crystalline ammonium dihydrogenphosphate to +2.5 ppm. The ^{13}C CPMAS spectra were recorded using a recycle time of 5 s, contact times of 1 ms, spinning rates of 7 kHz. Both ^{31}P and ^{13}C solid-state NMR spectra were recorded at room temperature and were transformed using a line broadening of 20 Hz. The number of scans (NS) are indicated in the figure captions.

3.2. Synthesis of species 5–8

3.2.1. Synthesis of 5

To a suspension of the Lawesson's reagent $[S_2P(\mu\text{-}C_6H_4\text{-}OMe)]_2$ (0.404 g; 1.0 mmol) in wet toluene (15 ml), pyrazole was added (0.680 g; 10.0 mmol). The reaction mixture was kept under stirring for 4 h at 333 K, then the white compound was filtered off, washed with toluene and dried under vacuum. IR (nujol): strong and broad absorption band at 1869 cm^{-1} assigned to hydrogen bonds of either the N–H···O, or, for the formulation reported in footnote 1, the N–H···N type [22,23]. *Anal.* Calc. for $C_{13}H_{17}N_4O_2PS_2$ (356.4 g mol^{-1}): C, 43.81; H, 4.81; N, 15.72. Found: C, 44.12; H, 4.67; N, 15.76%. δ_H (400 MHz; CD_3COCD_3; Me_4Si) 9.3 (1H, b s, N–H/O–H), 7.99 (2H, m, Ph), 7.76 (4H, s, $C(3,5)_{pz}$-H), 7.05 (2H, m, Ph), 6.33 (2H, s, $C(4)_{pz}$-H), 3.88 (3H, s, OCH_3) – δ_C (100 MHz; CD_3COCD_3; Me_4Si) 162.7 (Ph), 133.6 ($C_{pz}(3,5)$), 132.7 (Ph), 113.8 (Ph), 105.0 [$C_{pz}(4)$], 55.4 (OCH_3) – δ_P (162 MHz; CD_3COCD_3; H_3PO_4) 78.6 (s) – δ_P (162 MHz; solid state): 97.3 (s), 94.5 (s).

3.2.2. Synthesis of 6

The Lawesson's reagent (0.404 g; 1.0 mmol) and pyrazole (0.680 g; 1.0 mmol) were heated at 75 °C in a sealed flask under nitrogen atmosphere and under stirring for 4 h. The mixture was then allowed to cool and solidify giving a white compound. The residue was then washed many times with anhydrous toluene in order to eliminate excess of pyrazole and to solidify the sample. δ_P (162 MHz; CD_3COCD_3; H_3PO_4) 72.8 (s) – δ_P (162 MHz; solid state): 82.3 (s).

3.2.3. Synthesis of 7

To a solution of $Ni(ClO_4)_2 \cdot 6H_2O$ (0.150 g; 4.2×10^{-1} mmol) in acetonitrile (4 ml), at room temperature and under inert atmosphere, species **5** (0.300 g; 8.4×10^{-1} mmol) was added in one portion. The reaction mixture was kept under stirring for 2 h, then filtered off, washed with acetonitrile and dried under vacuum (yield: 80.2%). IR (nujol): absorption at 1870 cm^{-1}. *Anal.* Calc. for $C_{20}H_{24}N_4O_4S_4P_2Ni$ (633.3 g mol^{-1}): C, 37.93; H, 3.82; N, 8.85. Found: C, 37.82; H, 3.73; N, 8.64%. δ_H (400 MHz; CD_3COCD_3; Me_4Si) 8.12 (2H, m, Ph), 7.12 (2H, m, Ph), 4.19 (1H, b s, N–H/O–H), 3.92 (3H, s, OCH_3) – δ_P (162 MHz; CD_3COCD_3; H_3PO_4) 85 (b s) – δ_P (162 MHz; solid state): 77.3 (s). Crystals suitable for

an X-ray structure determination were obtained by slow diffusion of dichloromethane into an acetone solution of **7**.

3.2.4. Synthesis of 8

To a stirred solution of $Ni(ClO_4)_2 \cdot 6H_2O$ (0.150 g; 4.2×10^{-1} mmol) in acetonitrile (4 ml) at room temperature and under inert atmosphere, **5** (300 g; 8.4×10^{-1} mmol) was added in one portion. After a couple of minutes, Et_3N (0.800 ml) was added dropwise. The brown solid formed was stirred under dinitrogen atmosphere for 2 h, then filtered out, washed with acetonitrile and acetone and dried under vacuum (yield: 84.3%). *Anal.* Calc. for $C_{26}H_{44}N_2O_4S_4P_2Ni$ (699.5 g mol^{-1}): C, 44.63; H, 6.58; N, 4.00. Found: C, 44.82; H, 6.66; N, 4.07%. δ_H (400 MHz; CD_3COCD_3; Me_4Si) 8.24 (2H, m, Ph), 6.98 (2H, m, Ph), 4.83 (1H, b s, N–H/O–H), 3.87 (3H, s, OCH_3), 3.28 (12 H, q, CH_2), 1.35 (18 H, t, CH_3) – δ_P (162 MHz; CD_3COCD_3; H_3PO_4) 69.4 (b s) – δ_P (162 MHz; solid state): 59.7 (s). Crystals suitable for an X-ray structure determination were obtained by slow diffusion of diethyl ether into a methanol solution of **8**.

3.3. X-ray crystallography

Species **7** and **8** crystallize as violet and brown single crystals suitable for X-ray diffraction. Crystals of approximate $0.20 \times 0.14 \times 0.06$ and $0.30 \times 0.20 \times 0.05$ mm dimensions (for **7** and **8**, respectively) were glued on the tip of a glass fibre and mounted on top of a goniometer head. The data were collected using graphite-monochromated Mo Kα radiation ($\lambda = 0.71073$ Å) on Bruker AXS SMART (**7**) or Enraf Nonius CAD-4 (**8**) automated diffractometers. In the first case, the unit cell was determined by acquiring 60 frames (44 reflections) at different ω and ϕ goniometer angles. In the latter, the unit cell was determined on the basis of the setting angles of 25 intense, randomly distributed, reflections with θ in the 9–12° range. A total of 9989 and 3254 reflections, in the $2.3° < \theta < 30.0°$ and $3.0° < \theta < 25.0°$ range (for **7** and **8**, respectively), were collected in the ω-scan mode [SMART: $\Delta\omega = 0.3°$; CAD-4: $\Delta\omega = 0.8 + (0.35\tan\theta)$]. Generator settings: 45 kV, 40 mA (SMART); 50 kV, 30 mA (CAD-4). The data were corrected for Lorenz-polarization and for absorption effects [24,25]. The structure solutions and refinements were performed by direct methods (SIR-97) [26] and full-matrix least-squares procedures on F^2 (SHELX-97) [27], respectively, as implemented in the WinGX suite of programs. All non-hydrogen atoms were treated anisotropically. Hydrogen atoms were made riding on the pertinent parent atoms with an isotropic thermal displacement parameter arbitrarily chosen as 1.2 times that of the parent atom itself. In the case of complex **7** both hydrogen atoms involved in the P–O–H–N hydrogen bond interactions were arbitrarily assigned to the nitrogen atoms. Further details of the crystal structure analyses can be found in Table 3.

Table 3
Crystallographic data and structure refinement parameters for species **7** and **8**

Compound	**7**	**8**
Method	single-crystal XRD	single-crystal XRD
Formula	$C_{20}H_{24}Ni_1N_4O_4P_2S_4$	$C_{26}H_{46}Ni_1N_2O_4P_2S_4$
Formula weight (g mol^{-1})	633.3	699.6
T (K)	298(2)	298(2)
λ (Å)	0.71073	0.71073
Crystal system	triclinic	triclinic
Space group	$P\bar{1}$	$P\bar{1}$
a (Å)	8.484(1)	7.719(3)
b (Å)	9.856(1)	9.122(3)
c (Å)	10.114(1)	13.220(1)
α (°)	109.217(2)	77.81(2)
β (°)	99.837(2)	87.79(2)
γ (°)	113.666(2)	71.70(3)
V (Å^3)	685.1(1)	863.5(4)
Z	1	1
ρ_{calc} (Mg m^{-3})	1.535	1.345
μ (mm^{-1})	1.164	0.928
$F(000)$	326	370
θ Range (°)	2.3–30.0	3.0–25.0
Collected hkl	$-11 \leqslant h \leqslant 11$, $-13 \leqslant k \leqslant 13$, $-14 \leqslant l \leqslant 14$	$0 \leqslant h \leqslant 9$, $-10 \leqslant k \leqslant 10$, $-15 \leqslant l \leqslant 15$
Measured/ independent reflections	9989/3970	3254/3010
Absorption corrections	empirical	empirical
Refinement method	full-matrix least-squares on F^2	full-matrix least-squares on F^2
Data/restrain/ parameter	3970/0/168	3010/0/182
$S(F^2)$[a]	0.900	1.018
$R(F)$, $wR(F^2)$[b] $[I > 2\sigma I]$	0.097, 0.122	0.059, 0.086
$R(F)$, $wR(F^2)$[b] (all)	0.047, 0.105	0.038, 0.078
Maximum and minimum $\Delta\rho$ (e Å^{-3})	0.96 and −0.57	0.40 and −0.26

[a] $S(F^2) = [\sum w(F_o^2 - F_c^2)^2/(n-p)]^{1/2}$ where n is the number of reflections, p the number of parameters and $w = 1/[\sigma^2(F_o^2) + (0.019P)^2 + 1.88P]$ with $P = (F_o^2 + 2F_c^2)/3$.

[b] $R(F) = \sum||F_o| - |F_c||/\sum|F_o|$ and $wR(F^2) = [\sum w(F_o^2 - F_c^2)^2/\sum wF_o^4]^{1/2}$.

4. Conclusions

The syntheses and spectroscopic characterization of the new, S-donor 4-methoxophenyldithiophosphonate ligand (L) have been described. Its coordination properties have been investigated towards the Ni(II) metal centre, and the structural characterization of two salts, containing the centrosymmetric *trans*-$[NiL_2]^{2-}$ anion, has been performed. The extensive solution and solid state multinuclear characterization has allowed to determine the nature of labile intermediates, which could neither be isolated as single crystals nor as *air stable* polycrystalline materials.

Work is in progress, aiming at obtaining distinct thiophosphonate salts of higher stability to be used in the

formation of new metal complexes, by employing differently substituted pyrazoles, and new characterization techniques, such as ab initio X-ray powder diffraction methods [28].

Acknowledgments

This work was supported by the Ministero dell'Università e della Ricerca (MIUR). We deeply thank Prof. N. Masciocchi, University of Insubria, for helpful discussions.

Appendix A. Supplementary material

Crystallographic data (excluding structure factors) for the two crystal phases have been deposited with the Cambridge Crystallographic Data Centre. CCDC 606670 and 606671 contain the supplementary crystallographic data for this paper. These data can be obtained free of charge via http://www.ccdc.cam.ac.uk/conts/retrieving.html, or from the Cambridge Crystallographic Data Centre, 12 Union Road, Cambridge CB2 1EZ, UK; fax: (+44) 1223-336-033; or e-mail: deposit@ccdc.cam.ac.uk. Supplementary data associated with this article can be found, in the online version, at doi:10.1016/j.poly.2006.09.077.

References

[1] N.K. Roy, Pesticides A 13 (1990) 1989.
[2] A.J. Burn, I. Gosney, C.P. Warrens, J.P. Wastle, J. Chem. Soc., Perkin Trans. 2 (1995) 265.
[3] C.C. Chavdarian, O-(substituted benzyl) dithiophosphonate insecticides. Stauffer Chemical Co., US Patent 4,683,225, 1987.
[4] C.C. Chavdarian, O-(substitued allylic) dithiophosphonate insecticides. Stauffer Chemical Co., US Patent 4,656,164, 1987.
[5] D. Klaman (Ed.), Lubrificants and Related Products, Verlag Chemie, Weinheim, 1984.
[6] J.M. Dumdum, L.T. Mendelson, R.L. Pilling, US Patent 4,908,142, 1990, Chem. Abstr. 112 (1990) 201925.
[7] I. Haiduc, D.B. Sowerby, S.F. Lu, Polyhedron 14 (1995) 3389.
[8] I. Haiduc, J. Organomet. Chem. 623 (2001) 29.
[9] P.G. Harrison, M.J. Begley, T. Kikabhai, F. Killer, J. Chem. Soc., Dalton Trans. (1986) 925.
[10] A.J. Burn, I. Gosney, C.P. Warres, J.P. Wastle, J. Chem. Soc., Perkin Trans. 2 (1995) 265.
[11] (a) E. Livingstone, A.E. Mikhelson, Inorg. Chem. 9 (1970) 2545;
(b) R. Engel, Chem. Rev. 77 (1976) 349;
(c) R. Engel, in: R.L. Heildebrand (Ed.), The Role of Phosphonates in Living System, CRC Press, Boca Raton, FL, 1983, p. 93;
(d) G.R.J. Thatcher, A.S. Campbell, J. Org. Chem. 58 (1993) 2272;
(e) M. de Fernandez, C.P. Vlaas, H. Fan, Y.H. Liu, F.R. Fronczek, R.P. Hammer, J. Org. Chem. 60 (1995) 7390.
[12] (a) W.E. van Zyl, J.P. Fackler, Phosphorus, Sulfur Silicon 167 (2000) 117;
(b) J.R. Wasson, G.M. Woltermann, H. Stoklosa, J. Fortschr. Chem. Forsch. (Top. Curr. Chem.) 35 (1973) 65;
(c) W. Kuchen, H. Hertel, Angew. Chem., Int. Ed. Engl. 8 (1969) 89;
(d) R.C. Mehrotra, G. Svrivastava, B.P.S. Chauhan, Coord. Chem. Rev. 55 (1984) 207.
[13] (a) B. Yed, N.M. Yousif, U. Pedersen, I. Thomsen, S.-O. Lawesson, Tetrahedron 40 (1984) 2047;
(b) S. Scheibye, R. Shabana, S.-O. Lawesson, Tetrahedron 38 (1982) 993.
[14] (a) V.G. Albano, M.C. Aragoni, M. Arca, C. Castellari, F. Demartin, F.A. Devillanova, F. Isaia, V. Lippolis, L. Loddo, G. Verani, Chem. Commun. (2002) 1170;
(b) M.C. Aragoni, M. Arca, F. Demartin, F.A. Devillanova, F. Isaia, V. Lippolis, G. Verani, Inorg. Chim. Acta 358 (2005) 213.
[15] A. Maspero, I. Kain, A.A. Mohamad, M.A. Omary, RJ. Staples, J.P. Fackler, Inorg. Chem. 42 (2003) 311.
[16] W.E. van Zyl, J.P. Fackler, Phosphorus, Sulfur Silicon 167 (2000) 117.
[17] Available from: <http://www.chem.wisc.edu/areas/reich/handouts/nmr-h/data157.gif>.
[18] K. Clausen, A.A. El-Barbary, S.-O. Lawesson, Tetrahedron 37 (1981) 1019.
[19] M.C. Aragoni, M. Arca, F. Demartin, F.A. Devillanova, G. Graiff, F. Isaia, V. Lippolis, A. Tiripicchio, G. Verani, Eur. J. Inorg. Chem. (2000) 2239.
[20] O. Hager, A.L. Llamas-Saiz, C. Foces-Foces, R.M. Claramunt, C. Lopez, J. Elguero, Helv. Chim. Acta 82 (1999) 2213.
[21] H.H. Limbach, G.S. Denisov, S. Golubev, in: A. Kohen, H.H. Limbach (Eds.), Hydrogen Bond Isotope Effects Studied by NMR, CRC Press/Taylor & Francis, Boca Raton, FL/London, 2005, p. 193 (Chapter 7).
[22] M.K. Ehlert, S.J. Rettig, A. Storr, R.C. Thompson, J. Trotter, Can. J. Chem. 68 (1990) 1494.
[23] M.K. Ehlert, S.J. Rettig, A. Storr, R.C. Thompson, J. Trotter, Can. J. Chem. 71 (1993) 1425.
[24] Complex **7**: G. Sheldrick, B. Blessing, Acta Crystallogr., Sect. A 51 (1995) 33.
[25] Complex **8**: A.C.T. North, D.C. Phillips, F.S. Mathews, Acta Crystallogr., Sect. A 24 (1968) 351.
[26] A. Altomare, M.C. Burla, M. Camalli, G.L. Cascarano, C. Giacovazzo, A. Guagliardi, A.G.G. Moliterni, G. Polidori, R. Spagna, J. Appl. Crystallogr. 32 (1999) 115.
[27] G.M. Sheldrick, SHELX-97: Program for Crystal Structure Determination, University of Göttingen, Göttingen, Germany, 1997.
[28] N. Masciocchi, S. Galli, A. Sironi, Comments Inorg. Chem. 26 (2005) 1.